

Parametrical study of the behavior of exterior unreinforced concrete beam-column joints through numerical modeling

Matheus F. A. Silva^{*1} and Vladimir G. Haach^{2a}

¹University of Sao Paulo, Department of Structures, Av. Trabalhador Saocarlense, 400, 13566-590, Sao Carlos – SP, BRAZIL

²University of Sao Paulo, Department of Structures, Av. Trabalhador Saocarlense, 400, 13566-590, Sao Carlos – SP, BRAZIL

(Received January 12, 2016, Revised February 15, 2016, Accepted April 15, 2016)

Abstract. Exterior beam-column joints are structural elements that ensure connection between beams and columns. The joint strength is generally assumed to be governed by the structural element of lowest load capacity (beam or column), however, the joint may be the weakest link. The joint shear behavior is still not well understood due to the influence of several variables, such as geometry of the connection, stress level in the column, concrete strength and longitudinal beam reinforcement. A parametrical study based only on experiments would be impracticable and not necessarily exposes the failure mechanisms. This paper reports on a set of numerical simulations conducted in DIANA[®] software for the investigation of the shear strength of exterior joints. The geometry of the joints and stress level on the column are the variables evaluated. Results have led to empirical expressions that provide the shear strength of unreinforced exterior beam-column joints.

Keywords: beam-column; shear; numerical analysis; parametrical analysis; reinforced concrete

1. Introduction

Joints are important regions of a concrete structure, as they ensure connection between beams and columns. The joint shear behavior is still not well understood due to the influence of several variables, such as column axial load, concrete strength, reinforcement details, and joint aspect ratio, among others. Besides, beam-column joints are regions of hard manufacture because of the large amount of reinforcement that converges to them (Ehsani and Wight 1985, 1990; Hwang *et al.* 2005; Lee and Yu 2009).

In the past, the member of lowest strength in a frame was believed to govern the beam-column joints strength (Park and Paulay 1975). Many valuable studies on this subject have been conducted and have indicated this is not always true. The formation of plastic hinges at the ends of a beam is the most desired structural behavior in case of a failure of connection. However, joints are often

*Corresponding author, Ph.D. Student, E-mail: matheusilva@usp.br

^aProfessor, Ph.D., E-mail: vghaach@sc.usp.br

the weakest links in a structural system. In tests conducted by Kuang and Wong (2006), a shear failure of a beam-column joint occurred when the beam had reached only half of its flexural capacity, i.e., when the beam was only under service loads.

Many experimental programs have focused on the study of the variables that interact to control the behavior of a joint (Haach *et al.* 2014; Hegger *et al.* 2003; Masi *et al.* 2013; Murty *et al.* 2003; Ortiz 1993; Sarsam and Phipps 1985; Scott 1992; Wong 2005) and showed this subject is quite complex. Marques and Jirsa (1972) also evaluated the effect of low column axial load and concluded its influence on the joint behavior was negligible. Hegger *et al.* (2003) showed normal stresses higher than 40% of the concrete compressive strength could reduce the joint shear strength. Corroborating with Hegger *et al.* (2003), Haach *et al.* (2014) experimentally investigated the influence of the column axial load on the shear behavior of the exterior joint. Three identical models of beam column joints (joint aspect ratio = $h_b/h_c = 1.58$) with different levels of axial load were analyzed ($v = 0.50, 0.65$ and 0.87). The authors observed an increase in the column axial load decreases the shear strength of the exterior joints. Haach *et al.* (2008) evaluated the behavior of exterior beam-column joints numerically and concluded the column axial load generated tension stresses on the beam longitudinal reinforcement and increased the shear force in the joint core. They also observed the eccentricity of the column axial load did not produce significant changes in the joint stress behavior.

Clyde *et al.* (2000) and Pantelides *et al.* (2002) reported a beneficial effect of the column axial load ($v = 0.1$ and 0.25) in the joint shear strength. Of the six specimens tested in Pantelides *et al.* (2002), the joint shear strength increased up to 15% by increasing v from 0.1 to 0.25 with a joint shear failure.

Hamil (2000) analyzed the influence of the joint aspect ratio of the beam-column joint and observed it exerted no influence on the initial joint cracking. However, the shear strength of the joint decreases with the increase in the geometric relationship, as pointed out by Vollum and Newman (1999). Park and Mosalam (2012) observed the same behavior and concluded it was related to the angle of inclination of the strut generated in the beam-column joint. Vollum and Newman (1999) believe few data have been published for a conclusive establishment of the joint aspect ratio influence, because it is difficult, if not impossible, to isolate such an influence from the other variables. On the other hand, Kim *et al.* (2009) constructed a database of experimental results of exterior joints of aspect ratios between 1.0 and 1.6 and observed a small reduction in the shear strength of the beam-column joints with the increase in the joint aspect ratio.

Due to the complex behavior of exterior beam-column joints, several design equations for predicting their shear strength have been proposed. Bakir and Boduroglu (2002) developed a model based on a parametric investigation. They evaluated 58 experimental results observing the main variables that influenced the joint behavior. Hwang and Lee (1999) proposed a model to predict the shear strength of exterior joints based on equilibrium and compatibility equations and constitutive laws of the cracked concrete. It considers relation h_b/h_c (inclination of strut), column axial load, joint hoop ratio and steel ratio of the intermediate column bars. Hegger *et al.* (2003) calibrated an empirical model using a database with more than 200 loaded tests to predict the failure for beam-column joints. Tsonos (2002) designed a simple model considering a uniform distribution of normal compressive stresses and shear stresses in the middle section of the joint. With this stress state, the author could recover the maximum principal stresses given by Mohr's circle. In general, these design equations assume each parameter has an isolated effect on the joint behavior (joint aspect ratio, column axial load, concrete strength and beam longitudinal reinforcement ratio). However, these parameters are interdependent, as observed by Vollum and

Newman (1999).

The number of specimens required on an experimental program for the development of a distinguished parametric study is normally impracticable. Several numerical studies have been performed in order to carry out parametrical studies on exterior beam-column joints (Abbas *et al.* 2014; Haach *et al.* 2008; Hegger *et al.* 2004; Masi *et al.* 2013). Therefore, a numerical modeling can provide valuable information, once several variations in the parameters that can influence their behavior can be evaluated at a low cost.

The present study is mostly concerned with the problem of the unreinforced external beam-column joint shear strength prediction by means of a unique expression. The proposed expression highlights the interaction between the joint aspect ratio and the column axial load. For this purpose, a 2D nonlinear finite element analysis were carried out using DIANA[®] software. The numerical model was validated through modeling tests conducted by Haach *et al.* (2014) and an extensive parametrical analysis was performed in DIANA[®] software. Then, the parametric studies were carried out through different joint aspect ratio coupled with increased column axial load. The influence of the two variables mentioned above were determined by a statistical analysis. Accuracy and uniformity of the final expression were assessed by comparing the model predictions with those of an experimental database.

2. Numerical modeling

The well-known commercial finite element software package DIANA[®] has been adopted for the nonlinear analysis of the beam-column joints. DIANA[®] is a well proven and tested software. The program includes an extensive material model library for concrete and analysis procedures. A Newton-Raphson iteration procedure was used with displacement control and an energetic convergence criterion of 10E-3 tolerance. After validation, the numerical model was used in a parametric study to further assess the influence of some parameters on the behavior of exterior beam-column joints.

2.1 Finite element mesh

Eight-node isoparametric plane stress distribution elements (CQ16M from Diana[®]2009a) with a Gauss integration scheme were adopted. The finite element mesh was defined with rectangular elements, maximum element aspect ratio of 2 and maximum size of elements ranging between 30 and 50 mm.

Reinforcement strains were computed from the displacement field of the continuum elements (structural elements), i.e., there was a perfect bond between the embedded reinforcement and the surrounding concrete.

2.2 Loading and boundary conditions

The configuration of the modeled specimens was defined to represent the resultant mechanical model of an exterior beam-column joint in a building, i.e., locate the connection between the points of the null bending moment, as indicated in Fig. (a). Therefore, in a numerical simulation, the ends of the column should be hinged whereas the load should be applied at the end of the cantilever beam, according to Fig. (b).

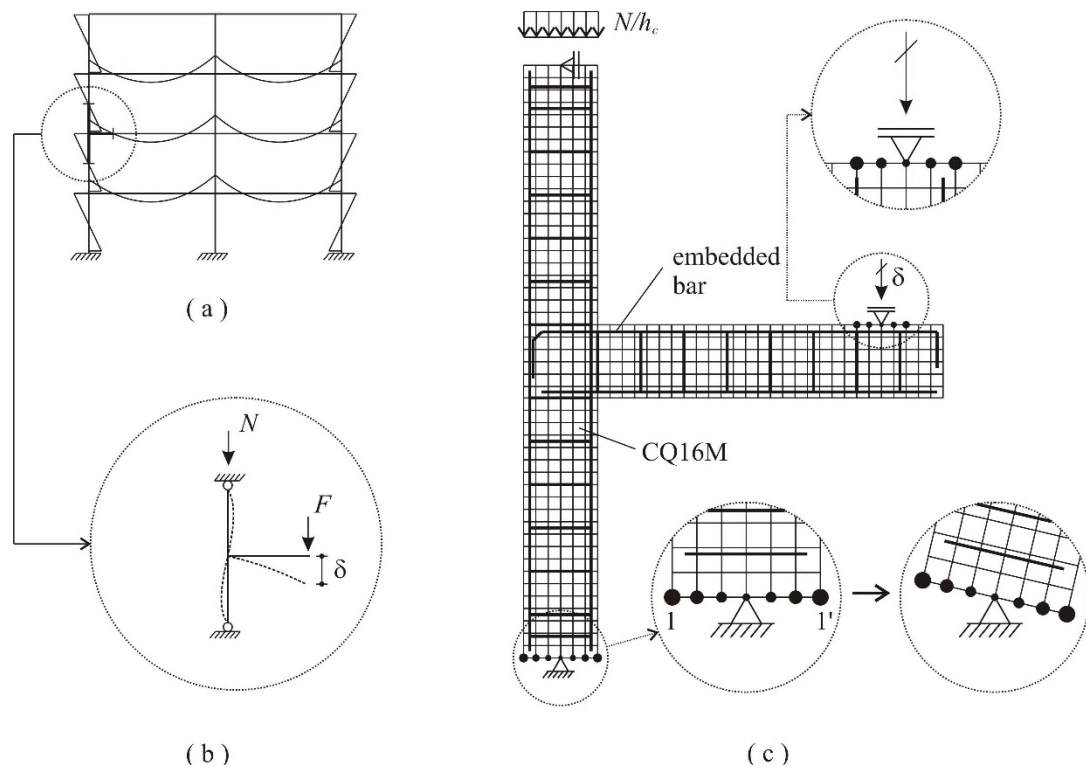


Fig. 1 Generic finite element model: (a) Bending moment diagram of a typical frame; (b) Frame model; (c) Loading and boundary conditions

In the numerical model, the top of the column was restricted to horizontal translations and the lower support was restricted to horizontal and vertical translations. The monotonic loading procedure was defined in two steps: firstly, a distributed load was applied at the top of the column until the desired axial level and kept constant until the end of the modeling; displacements were then applied to the beam extremity up to the failure of the numerical model.

Linear constraints were inserted in the finite element nodes neighboring the point of application of displacements of the beam for a better stress distribution, as shown in Fig. (c). This boundary condition considers a linear interpolation of the vertical displacements, i.e., slave nodes lie between two master nodes. Linear constraints were also inserted in the lower support of the column so that the section could remain plane and spin, see Fig. (c). In this case, the pairs of nodes of finite elements symmetrically located in relation to the axis of the column have the same absolute vertical displacement, but in opposite directions.

2.3 Material properties

The non-linear behavior of the concrete was represented by a Total Strain Crack Model based on a fixed stress vs. strain law concept available in DIANA[®] (2009b) software. The model describes the tensile and compressive behavior of the material with a stress \times strain relationship in a coordinate system fixed upon the cracking. Parabolic and linear constitutive laws were applied to describe the compressive and tensile behaviors of the concrete, respectively. The post-peak

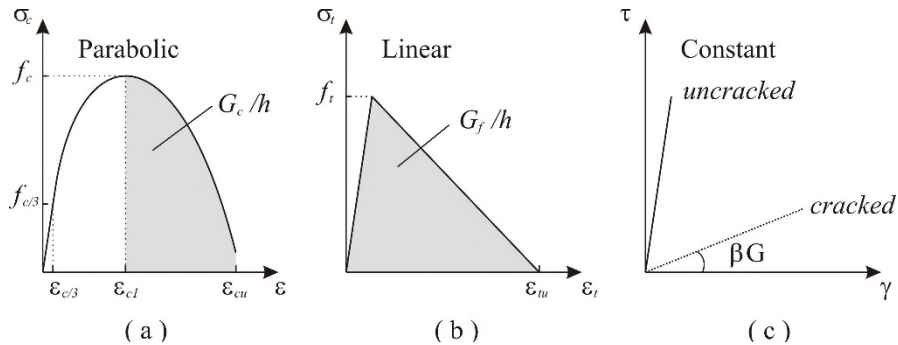


Fig. 2 Mechanical behavior of the concrete used in the numerical modeling: (a) Compression; (b) Tension and (c) Shear

behaviors were defined by the fracture energy under compression (G_c) and tension (G_f - Mode I), Fig. (a)-(b). Furthermore, a constant crack bandwidth (h) was adopted in simulations, according to Eq. (1).

$$h = \frac{2 \cdot G_f}{\epsilon_u \cdot f_t} \tag{1}$$

where ϵ_u is the ultimate tensile strain of the concrete and assumed equal to the yield strain of the reinforcement. The shear behavior during cracking was described through a shear retention model defined by a constant value, $\beta=0.2$, see Fig. 2(c).

A reduction factor to the compressive strength due to a lateral cracking of the concrete was considered based on Vecchio and Collins (1993). A confinement model for the concrete based on Selby and Vecchio (1993) was also considered, according to DIANA® (2009b). This model was used for the concrete and describes the increase in the compressive strength due to confinement. An elastic-plastic behavior was adopted for the reinforcement through the yield criterion of Von Mises.

3. Validation of the numerical model

The assessment of the influence of the geometry and column axial load on the joint was preceded by the validation of the numerical model adopted. Experimental model tested by Haach *et al.* (2014) (see Fig.) was numerically simulated for the comparison of experimental vs. numerical results. The experimental model was monotonically loaded until the failure of the joint. An axial load of 400kN was initially applied at the column corresponding to $\nu = 0.85$. Further details may be found at Haach *et al.* (2014).

The material properties of the model are listed in Table 1. The concrete compressive cylinder strength (f_c) and modulus of elasticity (E_c) were determined from experimental results reported in reference (Haach *et al.* 2014). The tensile strength and Mode-I fracture energy (G_f) were calculated according to CEB-FIP MC90 (1993).

The crack bandwidth was calculated by Eq. (1), where ϵ_u is the ultimate tensile strain of the concrete and assumed equal to the yield strain of a reinforcement with $f_y = 500$ MPa ($\epsilon_y = 500$

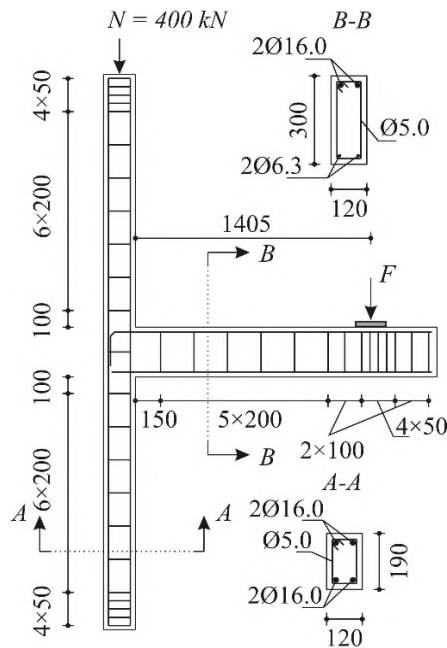
Fig. 3 Experimental model tested by Haach *et al.* (2014) Units in [mm]

Table 1 Mechanical properties of the materials

Concrete						
f_c (MPa)	f_t (MPa)	G_c (N/mm)	G_f (N/mm)	E_c (GPa)	β	h (mm)
22.36*	1.59*	0.561	0.053	25.46*	0.2	18.68
Steel						
Diameter (mm)	f_y (MPa)	E_s (GPa)		E_s (GPa)		
5.0	685.0	205.0		205.0		
6.3	563.0	205.0		205.0		
5.0	515.0	205.0		205.0		

*experimental data

MPa/ 210 GPa = 2.38‰).

According to DIANA[®] (2009b), the fracture energy under compression (G_c/h) is determined by the area under post peak stress strain. Therefore, the fracture energy and the crack bandwidth govern the post peak behavior of the concrete in compression. For this model, the fracture energy was calculated considering an ultimate compressive strain $\epsilon_{cu} = 3.5\%$.

The comparison between numerical and experimental load vs. displacement curves is shown in Fig. 4. In general, there was good agreement between the failure load obtained from the FE analysis and experimental test. For the numerical model, the failure was caused by an intense cracking of the concrete along the diagonal of the joint. The relations between the ultimate vertical load obtained from the finite element model and the experimental test was 0.89.

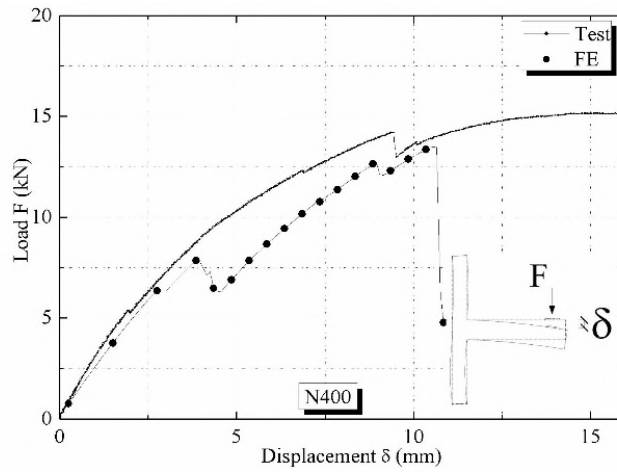


Fig. 4 Load-displacement curve of finite element and test results

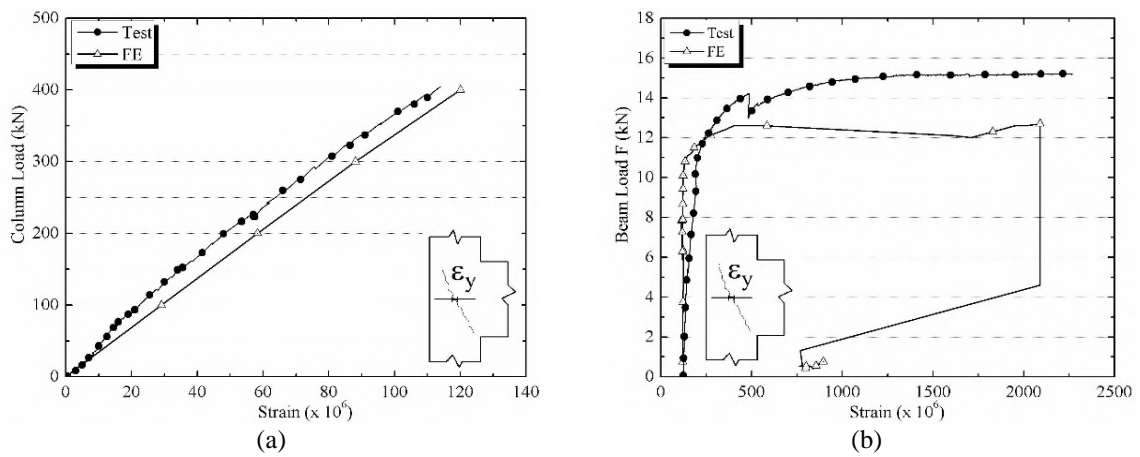


Fig. 5 Strain of stirrup inside the joint for N400: (a) Column Loading; (b) Beam Loading

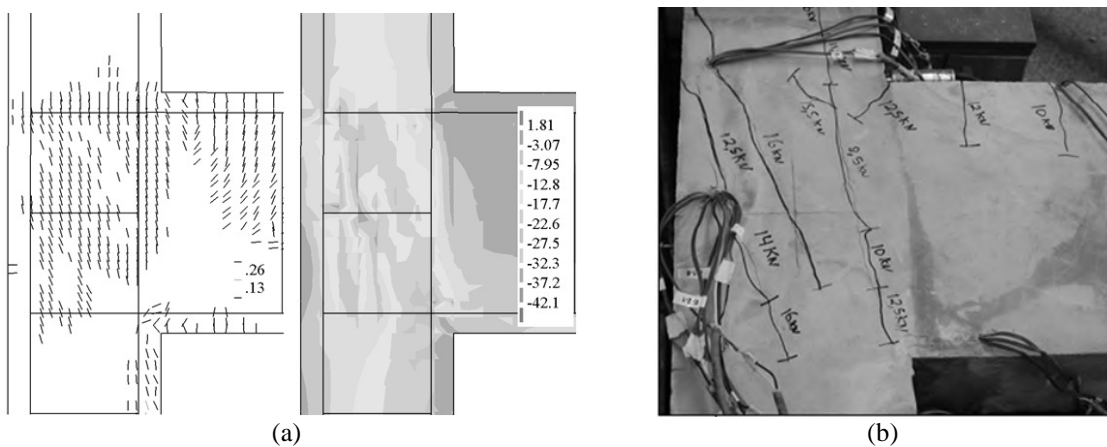


Fig. 6 Joint detail for the N400 model: (a) Cracks and Principal compressive stress in the numerical model and (b) cracks in the experimental model

In the N400 model tested by Haach *et al.* (2014), the strains in the middle of the stirrup located in the joint were very similar to the numerical results at the column loading, see Fig. 5(a). Initially, there was a good correlation between the FE and test strains at the beam loading. The behavior of the joint hoop after joint cracking ($\varepsilon_y \approx 0.25 \text{ ‰}$) was somewhat different. After cracking, the increase in the load caused cracks in the interior of the joint and the stirrup began to show significant strains, according to Fig. 5(b). Severe concrete damage was observed in this region, see Fig. 6.

In general, the numerical model has represented the global behavior of the experimental tests adequately; therefore, it is suitable for use in a parametric analysis of unreinforced concrete beam-column joints.

4. Parametric study

FEA enables not only the replication of experimental results, but also the development of parametric studies. A parametric analysis was conducted and the effects of joint aspect ratio and column axial load were studied. The joint shear strength was assumed a function of $(f_c)^{1/2}$, as

Table 2 Mechanical properties of the concrete

f_c (MPa)	f_t (MPa)	G_c (N/mm)	G_f (N/mm)	E_c (GPa)	β	h (mm)	Poisson's Ratio
30.00	2.93	0.64	0.066	31.00	0.20	18.68	0.2

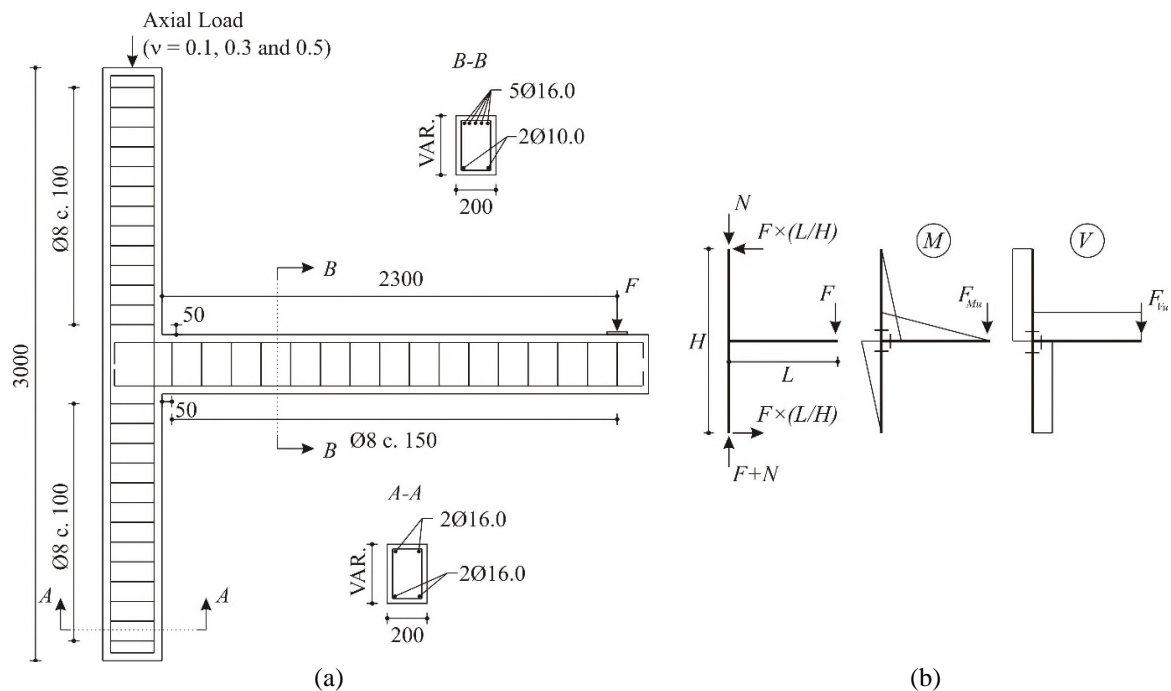


Fig. 7 Basic geometry of the parametric analysis. Units in [mm]

Table 3 Ultimate Force applied at the end of cantilever beam corresponding to Ultimate bending moment (F_{Mu}) and shear strength (F_{Vu}) of beam and column sections

Height of Member [mm]	Beam Section	Column Section		
		$v = 0.1$	$v = 0.3$	$v = 0.5$
200	-	$F_{Mu} = 31.91$ kN	$F_{Mu} = 41.91$ kN	$F_{Mu} = 37.07$ kN
		$F_{Vu} = 178.81$ kN	$F_{Vu} = 178.81$ kN	$F_{Vu} = 178.81$ kN
300	$F_{Mu} = 48.72$ kN	$F_{Mu} = 60.67$ kN	$F_{Mu} = 85.02$ kN	$F_{Mu} = 77.70$ kN
	$F_{Vu} = 176.60$ kN	$F_{Vu} = 284.00$ kN	$F_{Vu} = 284.00$ kN	$F_{Vu} = 284.00$ kN
400	$F_{Mu} = 70.56$ kN	$F_{Mu} = 94.12$ kN	$F_{Mu} = 137.36$ kN	$F_{Mu} = 128.31$ kN
	$F_{Vu} = 242.01$ kN	$F_{Vu} = 389.18$ kN	$= 389.18$ kN	$F_{Vu} = 389.18$ kN
500	$F_{Mu} = 93.22$ kN	$F_{Mu} = 132.16$ kN	$F_{Mu} = 199.64$ kN	$F_{Mu} = 199.64$ kN
	$F_{Vu} = 307.42$ kN	$F_{Vu} = 494.36$ kN	$= 494.36$ kN	$F_{Vu} = 494.36$ kN
600	$F_{Mu} = 115.13$ kN	$F_{Mu} = 174.89$ kN	$F_{Mu} = 271.90$ kN	$F_{Mu} = 260.33$ kN
	$F_{Vu} = 372.83$ kN	$F_{Vu} = 599.54$ kN	$= 599.54$ kN	$F_{Vu} = 599.54$ kN
700	$F_{Mu} = 137.77$ kN	-	-	-
	$F_{Vu} = 438.24$ kN	-	-	-

observed by (Bakir and Boduroglu 2002; Hamil 2000; Tsonos 2007; Vollum and Newman 1999).

According to (Bakir and Boduroglu 2002; Hegger *et al.* 2003; Vollum and Newman 1999), the shear strength of the beam-column joints decreases as the aspect ratio increases. Therefore, 25 joint aspect ratios were considered in the evaluation of the influence of this parameter on the behavior of beam-column joints. The basic geometry of the models is shown in Fig. 7(a). Five different heights of the beam ($h_b = 300, 400, 500, 600$ and 700 mm) and the column ($h_c = 200, 300, 400, 500$ and 600 mm) were modeled.

The previous considerations were adopted for the material models in the analysis. The yield stress, modulus of elasticity and Poissons's ratio of the steel bars were considered equal to 500 MPa, 210 GPa and 0.3, respectively. The mechanical properties applied to the concrete are listed in Table 2.

During the parametric study, the normalized axial stress applied to the column ($v = \sigma_c/f_c$) was kept equal to 0.1. Ultimate forces applied at the cantilever beam (F) are presented in Table . All models showed failure of the joint. Table shows the force applied to the beam for the achievement of the ultimate moment (F_{Mu}) and shear strength (F_{Vu}) of the beam and column, according to Fig. 7(b). The ultimate moments were calculated based on equilibrium and compatibility of section. Furthermore, nonlinear constitutive laws of concrete and elastic-plastic behavior for steel were adopted. In this way, Table corroborates the statements that all numerical models showed failure of the joint since the ultimate force applied at the beam was always less than beam or column failure loads ($F < F_{Mu}$ and $F < F_{Vu}$).

According to Table 4, three main joint failure modes were observed: diagonal cracking of the beam-column joint (failure mode A – Fig. 8), failure of the corner between the beam and the column in the horizontal direction (direction of beam - failure mode B –Fig. 9) and vertical direction (direction of column – failure mode C –Fig. 10). A diagonal cracking was observed in models of intermediate joint aspect ratios, for example Fig. 8(c). Failure mode B was observed in models of small joint aspect ratios (h_b/h_c). The diagonal strut showed high compressive stresses in the corner near the beam. Failure mode C was observed in models of large joint aspect ratios (h_b/h_c). Differently from failure mode B, the failure in the corner occurred due to the high

Table 4 Parametric analysis of h_b/h_c for $\nu=0.1$

$\nu=0.1$	h_c (mm)					
	200	300	400	500	600	
h_b (mm)	300	15.37 kN A	25.82 kN A	28.87 kN B	29.36 kN B	30.51 kN B
	400	19.19 kN A	34.38 kN A	43.48 kN B	47.42 kN B	48.60 kN B
	500	25.09 kN A	39.29 kN A	58.36 kN A	65.08 kN B	67.87 kN B
	600	28.87 kN C	50.31 kN A	73.67 kN A	87.39 kN B	87.28 kN B
	700	29.90 kN C	57.56 kN C	85.69 kN A	103.30 kN B	110.00 kN B

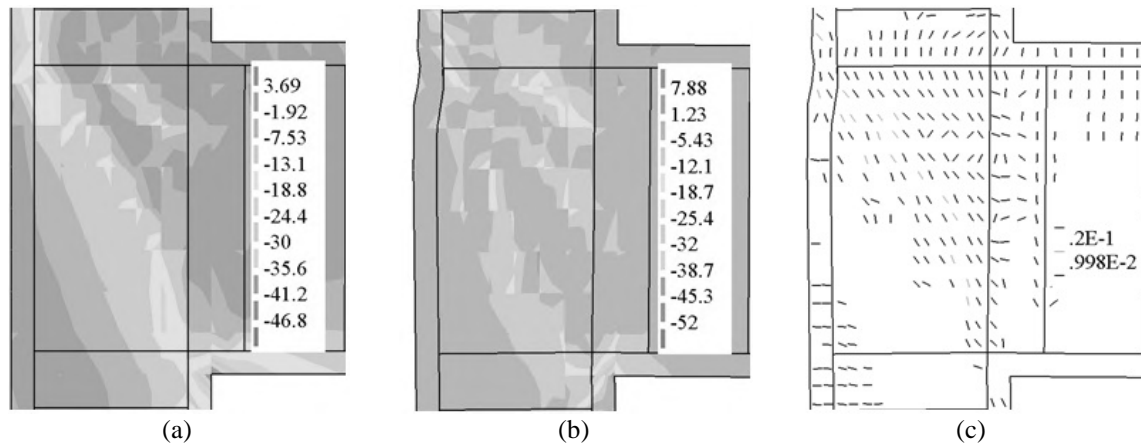


Fig. 8 Failure mechanism of 5030 obtained from the numerical modeling: (a) Contour plot of the principal compressive stress at the peak load; (b) Contour plot of the principal compressive stress after the peak load; (c) Crack pattern (smeared cracking) in the joint panel after the peak load

compressive stresses near the column. In fact, the reason for these failure modes (B and C) were related to the diagonal crushing of the joint in the corner, according to Fig. 9 (c) and Fig. 10(c), respectively.

Specimens of low- and high-joint aspect ratios showed generally a failure mode governed by compressive stresses. In low joint aspect ratios ($h_b/h_c < 1.40$), the low height of the beam promoted a concentration of stresses in the base of the beam-column joint in the compressed region of the beam. In the other case ($h_b/h_c > 2.33$), the low height of the column promoted a concentration of stresses in the base of the beam-column joint in the compressed region of the column. However, neither the beam nor the column reached their failure loads ($F < F_{Mu}$ and $F < F_{Vu}$), which indicates the failure of the beam-column joint.

For analysis purposes, the joint shear force V_{jh} was calculated according to Eq. (2).

$$V_{jh} = T_b - V_c \quad (2)$$

where T_b is the tensile force in the beam longitudinal bars and V_c is the column shear force.

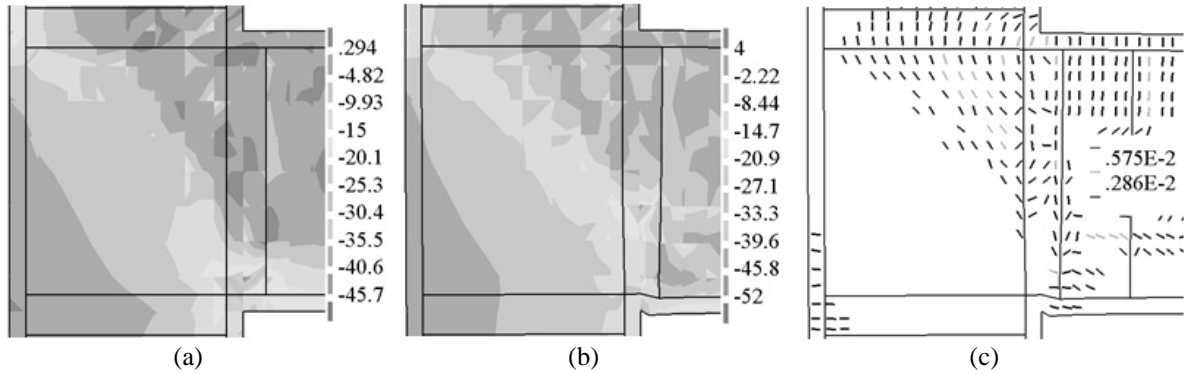


Fig. 9 Failure mechanism of 6050 obtained from the numerical modeling: (a) Contour plot of the principal compressive stress at the peak load; (b) Contour plot of the principal compressive stress after the peak load; (c) crack pattern (smeared cracking) in the joint panel after the peak load

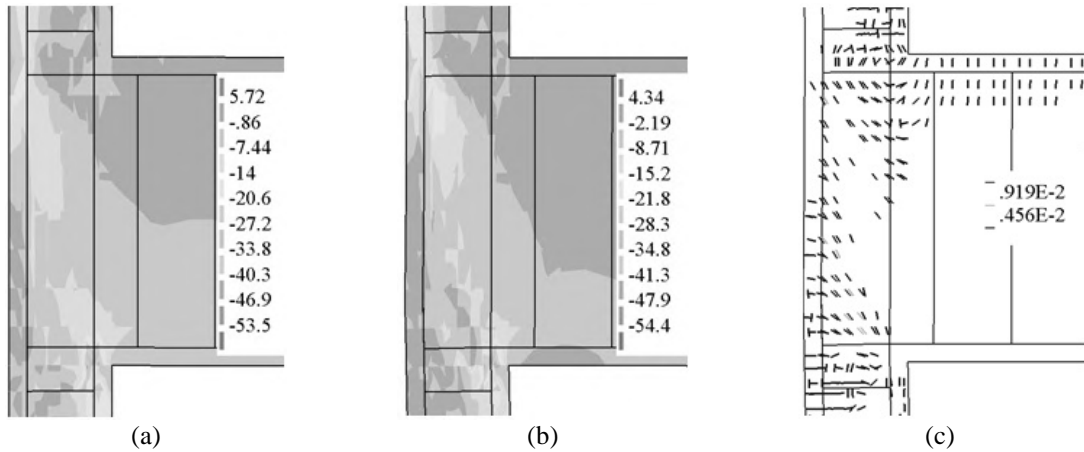


Fig. 10 Failure mechanism of 6020 obtained from the numerical modeling: (a) Contour plot of the principal compressive stress at the peak load; (b) Contour plot of the principal compressive stress after the peak load; (c) crack pattern (smeared cracking) in the joint panel after the peak load

The tensile force in the beam longitudinal bar was calculated as $\sigma_b \cdot A_{sb}$, where σ_b is the tension stress in the upper bar of the beam and A_{sb} is total area of this reinforcement (1005.31 mm²). The column shear force was calculated by the equilibrium of the numerical models, whose joint shear stress τ_{jh} was estimated according to Eq. (3).

$$\tau_{jh} = \frac{V_{jh}}{b_{eff} \cdot h_c} \quad (3)$$

where b_{eff} is the effective width of the joint = $(b_b + b_c)/2$, b_b is the width of the beam cross section; b_c and h_c is the width and height of the column cross section, respectively.

The effect of the joint aspect ratio (h_b/h_c) on the joint shear strength τ_{jh} is shown in Fig. . Only the numerical models with diagonal cracking at failure were included in the analysis. The shear strength was expressed as a function of $f_c^{0.5}$ and the joint aspect ratio is clearly related to $\tau_{jh}/f_c^{0.5}$, as

$$\frac{\tau_{jh}}{\sqrt{f_c}} = 0.86 - 0.2 \cdot \frac{h_b}{h_c} \quad (4)$$

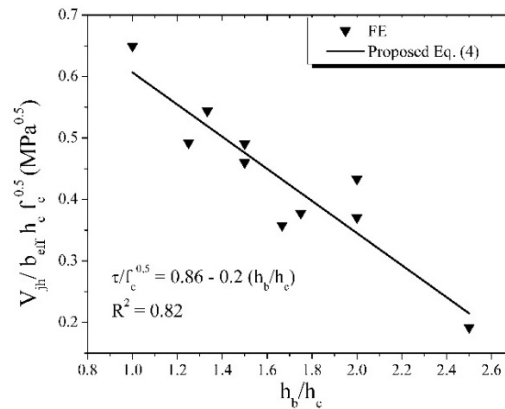


Fig. 11 Influence of the joint aspect ratio (h_b/h_c) on the joint shear strength

Table 5 Parametric analysis of h_b/h_c for $\nu=0.3$

$\nu=0.3$		h_c (mm)				
		200	300	400	500	600
h_b (mm)	300	20.32 kN	28.88 kN	30.12 kN	30.54 kN	31.22 kN
		A	B	B	B	B
	400	25.03 kN	43.42 kN	50.04 kN	51.02 kN	53.74 kN
		A	A	B	B	B
	500	30.19 kN	49.32 kN	68.07 kN	72.24 kN	73.13 kN
		C	A	B	B	B
	600	34.06 kN	60.44 kN	86.46 kN	98.91 kN	102.4 kN
		C	A	A	A	B
	700	35.77 kN	74.15 kN	109.8 kN	129.2 kN	121.1 kN
		C	A	A	A	B

shown in Eq. (4). By increasing h_b/h_c from 1.5 to 2.0, the shear strength decreased 18%, which is in agreement with the results of a parametric study conducted by Hegger *et al.* (2003).

The effect of the column axial load was investigated through the extrapolation of the column axial stress level shown in Table 4. Two additional levels of normalized axial stresses (ν) of 0.3 and 0.5 were analyzed (Table 5 and Table 6, respectively).

All the 50 additional models showed joint failure. Failure modes B and C were more frequent due to the increase in the axial stress in the column. As shown in Table 4 and Table 5, an increase in the column axial load (ν) from 0.1 to 0.3 causes an increase in the joint shear strength.

According to parametric studies of Hegger *et al.* (2004) and Baglin and Scott (2000), an increase in the normalized axial stress (ν) above 0.3 reduces the shear strength of the joint. Eight numerical models (Table 4) were chosen for detailing the influence of ν on different geometries

Table 6 Parametric analysis of h_b/h_c for $v=0.5$

$v=0.5$		h_c (mm)				
		200	300	400	500	600
h_b (mm)	300	20.23 kN A	31.01 kN B	37.34 kN B	38.93 kN B	32.62 kN B
	400	21.76 kN C	35.63 kN C	48.53 kN B	53.0 kN B	51.4 kN B
	500	25.88 kN C	52.39 kN A	70.30 kN B	76.99 kN B	73.50 kN B
	600	25.0 kN C	53.33 kN A	80.78 kN B	99.82 kN B	105.1 kN B
	700	27.71 kN C	54.40 kN C	93.35 kN C	105.3 kN C	119.9 kN C

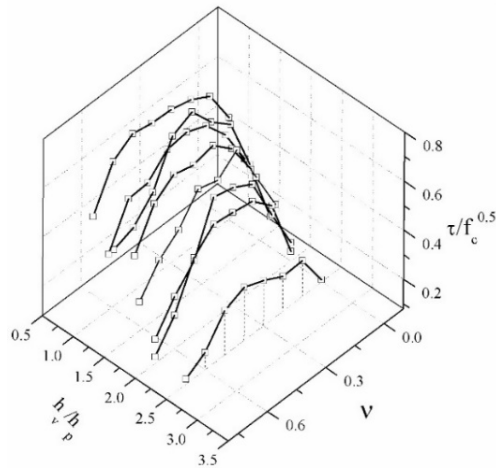


Fig. 12 Results of the parametric analysis of models 3030, 4020, 5020, 5030, 6030 and 7040

and the normalized axial stress ranged from 0 to 0.7 with 0.1 increments.

Apparently, there was a parabolic relationship between the shear strength and v (Fig. 12) for the same joint aspect ratio, which carry important implications for the behavior of beam-column joints. The shear strength moderately increased up to the level of normalized axial stress close to 0.35 and decreased linearly when the joint aspect ratio increased, as shown in Eq. (4). The beneficial effect of the column load up to level 0.35 was stronger for the models whose joint aspect ratio was higher than 1.67.

An equation that used a multiple regression of $\tau_{jh}/f_c^{0.5}$ (MPa^{0.5}) with independent variables h_b/h_c and v was proposed. A parabolic relation between the column axial load and the joint shear strength and a linear relation between the joint aspect ratio and the joint shear strength were considered, see Eq. (5).

$$\frac{\tau_{jh}}{\sqrt{f_c}} = (-1.51 \cdot \frac{h_b}{h_c} + 0.66) \cdot v^2 + (0.87 \cdot \frac{h_b}{h_c} - 0.11) \cdot v + (-0.24 \cdot \frac{h_b}{h_c} + 0.68) \quad (5)$$

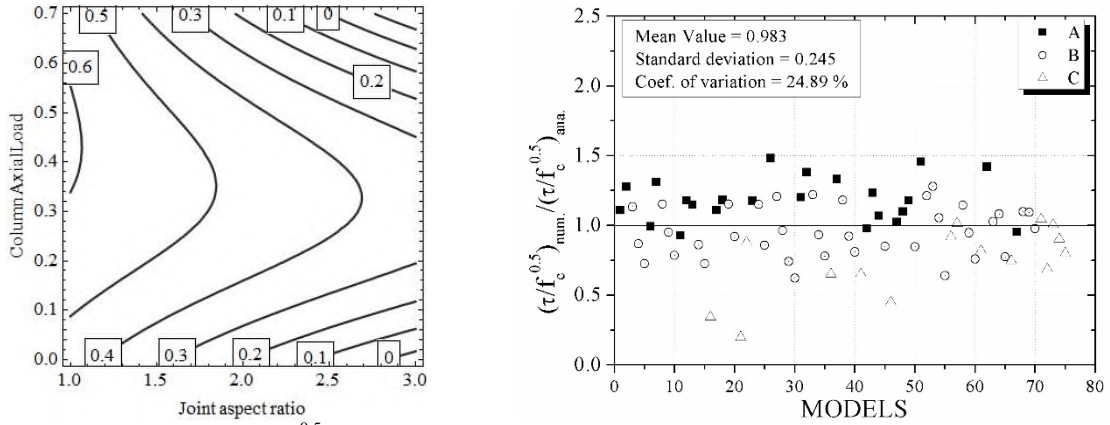


Fig. 13 (a) Contour plot of $\tau_{jh}/f_c^{0.5}$ in the adjusted equation; (b) Comparison between numerical results and normalized shear forces according to adjusted Eq.(5)

The normalized joint shear strength ($\tau_{jh}/f_c^{0.5}$), level of axial stress (ν) and h_b/h_c are plotted in Fig. 13(a). The joint shear strength clearly increased up to the level of normalized axial stress (ν) close to 0.35, at which it began to decline. Additionally, it showed decreasing values as h_b/h_c increased.

In Fig. 13(b) the numerical results of the 75 models are compared with those from Eq. (5). The statistical evaluation of the data resulted in a mean value of 0.983, standard deviation of 0.245, and coefficient of variation of 24.89%. These values show good agreement between Eq. (5) and the numerical results. Also, Fig. 13(b) depicts the failure modes (A, B and C) of the models.

5. Experimental verification

Eq. (6) for calculating the shear strength of exterior beam-column joints without transversal reinforcement was proposed based on Eq. (5) and the numerical results.

$$V_{jh} = b_{eff} h_c \sqrt{f_c} \cdot [(-1.51 \cdot \frac{h_b}{h_c} + 0.66) \cdot \nu^2 + (0.87 \cdot \frac{h_b}{h_c} - 0.11) \cdot \nu + (-0.24 \cdot \frac{h_b}{h_c} + 0.68)] \quad (6)$$

The test results from 34 exterior beam-column joints were used in the evaluation of the proposed model and comparison between its performance and the performance of the theoretical models proposed by Hwang and Lee (1999) Bakir and Boduroglu (2002), Tsonos (2007) and Hegger *et al.* (2003). Several exterior beam-column joints were collected from the literature for the database. Table 7 shows information about the literature sources from which the joints were taken. Tests with distinct geometries, concrete properties and column axial load were selected.

All the tests showed joint failure, since the ultimate moment and shear strength of the beams and columns were not reached. Only specimens with beam bars bent down into the column were collected, as they seem preferable regarding ductility in monotonic loading according to (Murty *et al.* 2003; Scott 1996).

In Fig. 14(a), the comparison between the experimental and theoretical ultimate shear strengths of the proposed model (V_{exp} / V_{theo}) is presented for the 34 tests of the database. The model

Table 7 Experimental database

N° of joints	Author
1-4	Ortiz (1993)
5-9	Parker and Bullman (1997)
10	Amoury and Ghobarah (2002)
11	Sarsam and Phipps (1985)
12	Scott and Hamill (1998)
13-16	Saravanan and Kumaran (2011)
17-20	Chaliores <i>et al.</i> (2008)
21	Murty <i>et al.</i> (2003)
22-23	Ghobarah and Said (2002)
24-26	Karayannis <i>et al.</i> (2007)
27-30	Clyde <i>et al.</i> (2000)
31-34	Wong and Kuang (2008)

achieved conservative values of the shear strength since only five models showed theoretical shear strength higher than the experimental values. The mean ratio between the experimental and theoretical shear strengths was approximately 1.49 and the coefficient of variation was equal to 34.81%.

Design models proposed by Hwang and Lee (1999) and Bakir and Boduroglu (2002) showed 1.0 as an approximate mean value of relation V_{exp} / V_{theo} , see Fig. 14(b) and Fig. 14(d), respectively. Design models proposed by Hegger *et al.* (2003) and Tsonos (2007) predicted higher shear strength values for most beam-column joints evaluated, see Fig. (c) and Fig. (e), respectively.

The complex behavior of the exterior beam-column joints hampers the definition of a design model that considers all variables. Hwang and Lee’s model is a very interesting theoretical design model, since it includes equilibrium conditions, strain compatibility and constitutive laws of materials. However, it does not take into account the influence of the longitudinal beam reinforcement ratio. Tsonos’ model is also very interesting because it uses the biaxial behavior of the concrete. However, as pointed out by Haach *et al.* (2014), it does not consider the column axial load influence, although the formulation is based on the equilibrium of normal and shear forces.

Hegger *et al.* (2003) proposed an empirical model that includes the influence of joint aspect ratio, column reinforcement ratio, normal stress in the column, compressive concrete strength, efficiency of the beam reinforcement anchorage and amount and efficiency of joint hoops. However, the database used in their study limits its application to some beam-column joints. Secondly, the design model of Hegger *et al.* (2003) demands a minimum joint hoop ratio, whereas the database only accounts for existing joints. Bakir and Boduroglu (2002) also proposed an empirical model considering the influence of several variables on the behavior of exterior beam-column joints. However, the authors found no evidences of the influence of normal stresses on the joint behavior.

The proposed design model considers only the influence of joint aspect ratio, concrete compressive strength and column axial load. Previous design models and several experimental studies available in the literature found longitudinal beam reinforcement exerts some influence on

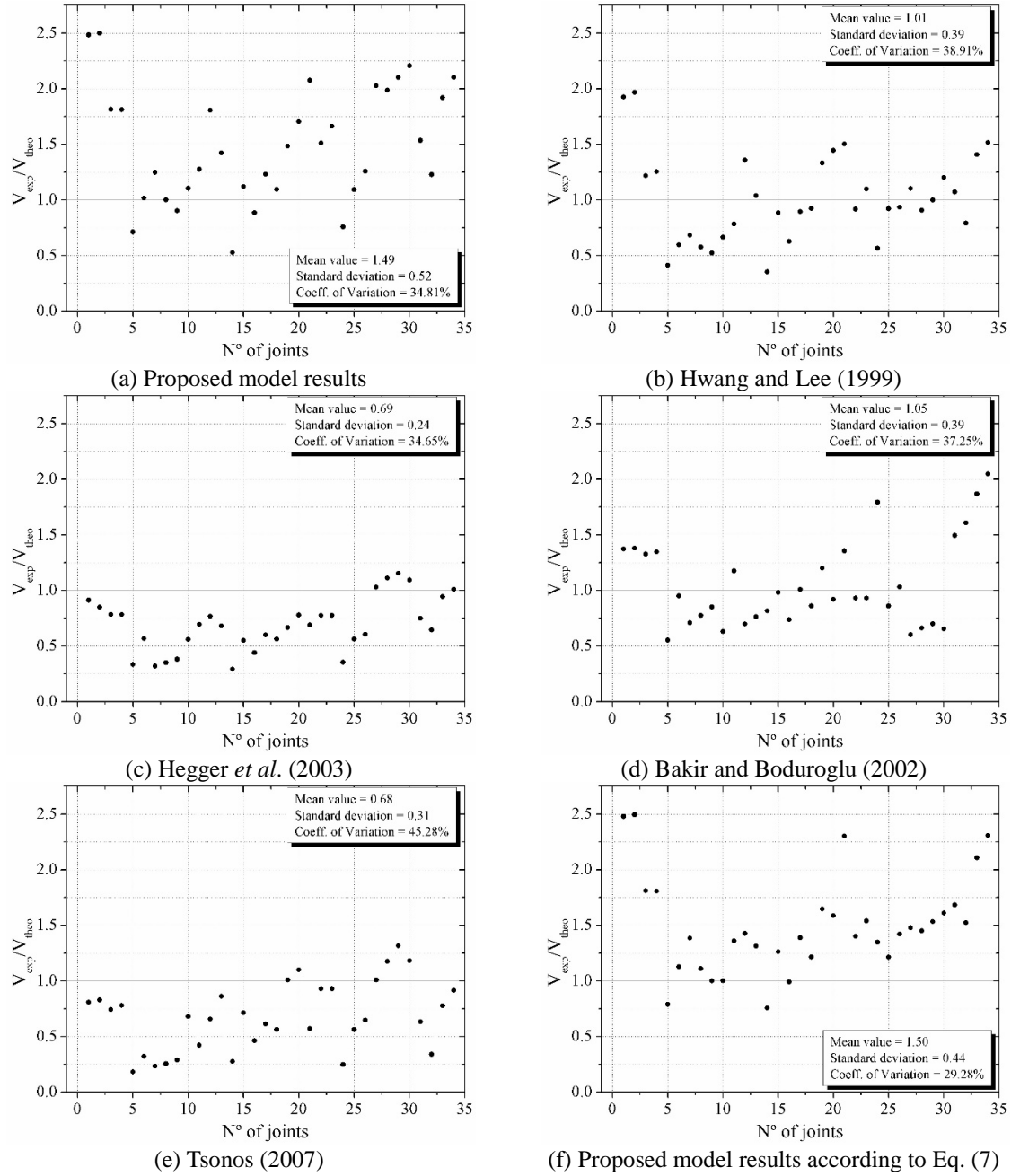


Fig. 14 Comparison between experimental and theoretical V_{exp} / V_{theo}

the behavior of beam-column joints. Since such reinforcement was not evaluated in the present numerical study, its contribution was added to the proposed model, as in Bakir and Boduroglu (2002) design model. Therefore, the modified shear strength V_{jh}^* is related to V_{jh} , from Eq. (6), by the following equation

$$V_{jh}^* = \left(\frac{100 \times A_{s,b}}{b_b \times h_b} \right)^{0.4289} \cdot V_{jh} \quad (7)$$

According to Fig. 14(f), there is a better correlation between the experimental strengths and the theoretical shear strengths based on Eq. (7). The mean ratio was approximately 1.50, with a 29.28% coefficient of variation. In comparison with other design models, the proposed model has shown the lowest coefficient of variation, whose mean value of relation (V_{exp}/V_{theo}) is higher than 1.0 and considered safe.

6. Conclusion and final remarks

A numerical study using DIANA® software and based on the finite element method was conducted for the evaluation of the behavior of exterior beam-column joints. FEM simulation were successfully applied to an experimental test. The FE's ultimate load and strains were compared with the experimental results of Haach *et al.* (2014) and good agreement was achieved. The validated results can be an effective tool for a better understanding of the failure mechanisms in beam column joints. A parametric study was also conducted and some parameters that influence the behavior of exterior beam-column joints were analyzed. Finally, a design model for exterior beam-column joints without transversal reinforcement has been proposed.

Concerning the results of the numerical modeling of exterior beam-column joints, the main following conclusions can be drawn:

- i) The results of FE simulations show the shear strength of unreinforced exterior beam-column joints decreases linearly with the increase in the joint aspect ratio. By increasing h_b/h_c from 1.5 to 2.0, the shear strength of the joint decreases 18%;
- ii) Three failure modes were observed: diagonal cracking, crushing of concrete in the joint-beam interface and crushing of concrete in the joint-column interface. The failure mode of the joints (A, B and C) is strongly affected by the joint aspect ratio and the column axial load;
- iii) The shear strength is affected by the interrelation between the joint aspect ratio and the column axial load, which shows the beneficial effect of the column axial load is greater to some joint aspect ratio;
- iv) The shear strength increased up to the level of normalized axial stress (ν) close to 0.35. A further increase in the column load resulted in a decrease in the shear strength;
- v) The statistical evaluation of the multiple regression resulted in 0.983 mean value of relation V_{num}/V_{theo} , standard deviation of 0.245, and coefficient of variation of 24.89%, which show good agreement between the adjusted Eq. (6) and the numerical results.

A database was used for the evaluation of Eq. (7) and conservative estimates were obtained. The mean ratio between the experimental and theoretical shear strengths was approximately 1.50, with a 29.28% coefficient of variation.

Acknowledgements

The authors gratefully acknowledge the funding provided by CAPES (Brazilian National Council for the Improvement of Higher Education).

References

- Abbas, A.A., Mohsin, S.M.S. and Cotsovos, D.M. (2014), “Seismic response of steel fibre reinforced concrete beam–column joints”, *Eng. Struct.*, **59**, 261-283.
- Baglin, P. and Scott, R. (2000), “Finite element modeling of reinforced concrete beam-column connections”, *ACI Struct. J.*, **97**(6), 886–894.
- Bakir, P.G. and Boduroğlu, H.M. (2002), “A new design equation for predicting the joint shear strength of monotonically loaded exterior beam-column joints”, *Eng. Struct.*, **24**(8), 1105-1117.
- Chalioris, C.E., Favvata, M.J. and Karayannis, C.G. (2008), “Reinforced concrete beam–column joints with crossed inclined bars under cyclic deformations”, *Earthq. Eng. Struct. Dy.*, **37**(6), 881-897.
- Clyde, C., Pantelides, C.P. and Reaveley, L.D. (2000), “Performance-Based Evaluation of Exterior Reinforced Concrete Building Joints for Seismic Excitation”, PEER Report 2000/05; University of California, Berkeley.
- COMITÉ EURO-INTERNATIONAL DU BÉTON (1993), Model Code 1990. MC-90. CEB-FIP, Bulletin D’Information, n.204.
- DIANA (2009a), *DIANA finite element analysis, User’s manual release 9*, Element library, Delft, Netherland: TNO DIANA.
- DIANA (2009b), *DIANA finite element analysis, User’s manual release 9*, Material library, Delft, Netherland: TNO DIANA.
- Ehsani, M.R. and Wight, J.K. (1985), “Exterior reinforced concrete beam-to-column connections subjected to earthquake-type loading”, *J. Proceedings*, **82**(4), 492-499.
- Ehsani, M.R. and Wight, J.K. (1990), “Confinement steel requirements for connections in ductile frames”, *J. Struct. Eng.*, **116**(3), 751-767.
- El-Amoury, T. and Ghobarah, A. (2002), “Seismic rehabilitation of beam–column joint using GFRP sheets”, *Eng. Struct.*, **24**(11), 1397-1407.
- Ghobarah, A. and Said, A. (2002), “Shear strengthening of beam-column joints”, *Eng. Struct.*, **24**(7), 881-888.
- Haach, V.G., El, A.L.H.D.C. and El Debs, M.K. (2008), “Evaluation of the influence of the column axial load on the behavior of monotonically loaded R/C exterior beam–column joints through numerical simulations”, *Eng. Struct.*, **30**(4), 965-975.
- Haach, V.G., El, A.L.H.D.C. and El Debs, M.K. (2014), “Influence of high column axial loads in exterior R/C beam-column joints”, *J. Civil Eng.*, **18**(2), 558-565.
- Hamil, S.J. (2000), “Reinforced concrete beam-column connection behavior”, Ph.D thesis; Durham University, UK.
- Hegger, J., Sherif, A. and Roeser, W. (2003), “Nonseismic design of beam-column joints”, *Struct. J.*, **100**(5), 654-664.
- Hegger, J., Sherif, A. and Roeser, W. (2004), “Nonlinear finite element analysis of reinforced concrete beam-column connections”, *Struct. J.*, **101**(5), 604-614.
- Hwang, S.J. and Lee, H.J. (1999), “Analytical model for predicting shear strengths of exterior reinforced concrete beam-column joints for seismic resistance”, *Struct. J.*, **96**(5), 846-858.
- Hwang, S.J., Lee, H.J., Liao, T.F., Wang, K.C. and Tsai, H.H. (2005), “Role of hoops on shear strength of reinforced concrete beam-column joints”, *ACI Struct. J.-American Concrete Inst.*, **102**(3), 445-453.
- Karayannis, C.G., Chalioris, C.E. and Sirkelis, G.M. (2008), “Local retrofit of exterior RC beam–column joints using thin RC jackets—An experimental study”, *Earthq. Eng. Struct. Dy.*, **37**(5), 727-746.
- Kim, J., LaFave, J.M. and Song, J. (2009), “Joint shear behaviour of reinforced concrete beam–column connections”, *Mag. Concrete Res.*, **61**(2), 119-132.
- Kuang, J.S. and Wong, H.F. (2006), “Effects of beam bar anchorage on beam-column joint behaviour”, *Proceedings of the Institution of Civil Engineers-Structures and Buildings*, **159**(2), 115-124.
- Lee, H.J. and Yu, S.Y. (2009), “Cyclic response of exterior beam-column joints with different anchorage methods”, *ACI Struct. J.*, **106**(3), 329.

- Marques, J. and Jirsa, J. (1972), "A study of hooked bar anchorages in beam-column joints", Research Report Number No. 33. Final Report; University of Texas, Austin.
- Masi, A., Santarsiero, G., Lignola, G.P. and Verderame, G.M. (2013), "Study of the seismic behavior of external RC beam-column joints through experimental tests and numerical simulations", *Eng. Struct.*, **52**, 207-219.
- Murty, C.V.R. (2003), "Effectiveness of reinforcement details in exterior reinforced concrete beam-column joints for earthquake resistance", *ACI Struct. J.*, **2**, 149-156.
- Ortiz, I.R. (1993), "Strut-and-Tie modeling of reinforced concrete. Short beams and beam-column joints", Ph.D. Thesis; University of Westminster, London, UK.
- Pantelides, C.P., Hansen, J. and Reaveley, L.D. (2002), "Assessment of reinforced concrete building exterior joints with standard details", PEER Report 2002/18; University of California, Berkeley.
- Park, R. and Paulay, T. (1975), *Reinforced concrete structures*, Wiley Interscience, New York, NY, USA.
- Park, S. and Mosalam, K.M. (2012), "Parameters for shear strength prediction of exterior beam-column joints without transverse reinforcement", *Eng. Struct.*, **36**, 198-209.
- Parker, D.E. and Bullman, P.J.M. (1997), "Shear strength within reinforced concrete beam-column joints", *Struct. Eng.*, **75**(4).
- Saravanan, J. and Kumaran, G. (2011), "Joint shear strength of FRP reinforced concrete beam-column joints", *Central Eur. J. Eng.*, **1**(1), 89-102.
- Sarsam, K. and Phipps, M. (1985), "The shear design of in situ reinforced concrete beam-column joints subjected to monotonic loading", *Mag. Concrete Res.*, **37**(130), 16-28.
- Scott, R. (1992), "The effects of detailing on RC beam/column connection behavior", *Struct. Eng.*, **70**(18), 318-324.
- Scott, R. (1996), "Intrinsic mechanisms in reinforced concrete beam-column connection behavior", *ACI Struct. J.*, **93**(3), 1-11.
- Scott, R.H. and Hamill, S.J. (1998), "Connection zone strain in reinforced concrete beam column connections", *Proceedings of the 11th International Conference on Experimental Mechanics*, 65-69.
- Selby, R.G. and Vecchio, F.J. (1993), "Three dimensional constitutive relations for reinforced concrete", Department of Civil Engineering, University of Toronto, Toronto, Canada, Publication No. 93-02.
- Tsonos, A. (2007), "Cyclic load behavior of reinforced concrete beam-column subassemblages of modern structures", *ACI Struct. J.*, **104**(4), 468-478.
- Tsonos, A.G. (2002), "Seismic repair of reinforced concrete beam column subassemblages of modern structures by epoxy injection technique", *Struct. Eng. Mech.*, **14**(5), 543-563.
- Vecchio, F. and Collins, M. (1993), "Compression response of cracked reinforced concrete", *J. Struct. Eng.*, **119**(12), 3590-3610.
- Vollum, R.L. and Newman, J.B. (1999), "The design of external, reinforced concrete beam-column joints", *Struct. Eng.*, **77**(23 and 24), 21-27.
- Wong, H. (2005), "Shear strength and seismic performance of non-seismically designed reinforced concrete beam-column joints", Ph.D. Thesis; The Hong Kong University of Science and Technology.
- Wong, H.F. and Kuang, J.S. (2008), "Effects of beam-column depth ratio on joint seismic behaviour", *Proceedings of the ICE-Structures and Buildings*, **161**(SB2), 91-101.

